Nature Environment and Pollution Technology
An International Quarterly Scientific Journal

p-ISSN: 0972-6268
(Print copies up to 2016)
e-ISSN: 2395-3454

Vol. 22 | No. 3 | pp. 1563-1569 | 2023

Original Research Paper

https://doi.org/10.46488/NEPT.2023.v22i03.042

Open Access Journal

Study on the Adsorption Properties of Cr(VI) by Biochar with Different Treatments

X. Zhang*†
*Department of International Education, Beijing University of Chemical Technology, Beijing 100029, P. R. China
†Corresponding authors: Xinyu Zhang; 1691748468@qq.com

Nat. Env. & Poll. Tech.
Website: www.neptjournal.com

Received: 13-02-2023
Revised: 24-03-2023
Accepted: 28-03-2023

Key Words:
Biochar
Cr(VI)
Kinetics
Thermodynamics,
Adsorption mechanism

ABSTRACT

The paper investigated the adsorption of Cr(VI) on biochar in simulated wastewater by static adsorption method, Fourier Transform Infrared spectra (FTIR), Raman, X-ray photoelectron spectroscopy (XPS), scanning electron microscope (SEM), and transmission electron microscope (TEM) characterization analysis. The results show that biochar can effectively remove Cr(VI) in wastewater, and the adsorption equilibrium can be quickly reached within 100 min. The kinetic analysis shows that the quasi-second-order kinetic model can better fit the kinetic process of Cr(VI) adsorption by biochar, which shows that the main mechanism of the adsorption is the chemical bonding cooperation between Cr(VI) and the functional groups on the surface of biochar. Fit analysis of the isotherm at different temperatures shows that temperature increase promotes the adsorption of Cr(VI) on biochar, and thermodynamic analysis reveals that the adsorption of Cr(VI) on biochar is a spontaneous endothermic process. The Freundlich model effectively fits the adsorption isotherm of Cr(VI), indicating that the surface of biochar is uneven and Cr(VI) has undergone multilayer adsorption. The adsorption isotherm of Cr(VI) under the influence of HA and FA can be effectively fitted by the Freundlich model, and the adsorption efficiency is the highest when FA is added. The national analysis of Fourier Transform Infrared spectra (FTIR), Raman, X-ray photoelectron spectroscopy (XPS), scanning electron microscope (SEM), and transmission electron microscope (TEM) further reveals the bond cooperation between Cr(VI) and the surface functional groups of biochar. The results show that biochar has potential application value in treating chrome-containing wastewater.

INTRODUCTION

With the rapid development of industry and commerce, a large amount of chromium-containing wastewater is produced in industrial production processes such as metal smelting, electroplating, tanning, printing, and dyeing, which is discharged into natural water bodies, seriously polluting the soil and groundwater environment (Zou et al. 2021). In nature, the main valence states of chromium (Cr) are trivalent and hexavalent, among which the compounds of chrome (Cr(VI)) are usually highly water-soluble and usually present in the form of CrO_4^{2-} and $Cr_2O_7^{2-}$ in the wastewater. With high toxicity, carcinogenicity, mutagenicity, and teratogenicity, Cr(VI) is hundreds of times more toxic than Cr(III), which may cause many serious health problems (Chen et al. 2018). Therefore, efficient and environmentally friendly methods are urgently needed to restore Cr(VI) in the environment.

Nowadays, the treatment of chrome-containing wastewater is mainly about physical and chemical methods, including chemical precipitation, ion exchange, flocculation, membrane treatment, adsorption, and so on. Adsorption is an efficient treatment method to remove heavy metal pollutants in water, usually using carbon adsorbents, clay mineral adsorbents, and adsorption resins (Wang et al. 2022). As a pore-rich carbon material formed under high temperatures and the conditions of hypoxia or no oxygen, biochar has the characteristics of high specific surface area, abundant surface active functional groups, and strong ion exchangeability, showing great development potential in the field of heavy metal pollution remediation (Mian & Liu 2018). Lyu et al. (2017, 2018) studied the removal of hexavalent chromium from aqueous solutions and in contaminated soils by a novel biochar-supported nanoscale iron sulfide composite. Herein, this paper selects biochar as the adsorbent of Cr(VI) in simulated wastewater and studies the effects of initial Cr(VI) concentration, reaction temperature, humic acid (HA), fulvic acid (FA), and other factors on the adsorption of Cr(VI) by biochar, conduct adsorption kinetics, adsorption isotherm, and material characterization analysis, and explore the mechanism of Cr(VI) adsorption by biochar and its potential application value in the treatment of chrome-containing wastewater.

MATERIALS AND METHODS

Experimental Materials and Instruments

The chemicals used in the experiment, such as potassium dichromate, diphenylcarbazide, sulfuric acid, hydrochloric acid, ethanol, sodium hydroxide, etc., are all commercially available analytical reagents. No purification treatment was done before use, and all solutions were prepared with deionized water. Some of the instruments used are as follows: pH meter (Five Easy plus, Mettler-Tollidor Instrument (Shanghai) Co., LTD.), Table type Low-temperature Constant Temperature Oscillating Shaker (PSE-T150A, Stoker Instrument Equipment (Shanghai) Co., LTD.), Electronic balance (AL204, Mettler-Tollidor Instrument (Shanghai) Co., LTD.), Uv-visible spectrophotometer (SP-756-P(scanning type), Shanghai spectrometer Co., LTD.), drum heating constant temperature drying oven (DHG-9053A, Shanghai sanfa scientific instrument Co., LTD.), automatic micro confocal Raman spectrometer (XploRA PLUS, Horiba France SAS Co., LTD.) France), Fourier Transform Infrared spectrometer (NICOLET6700, Thermo Scientific).

Adsorption Experiments

Adsorption of Cr(VI) by biochar: Under different reaction conditions (reaction time, HA, FA, temperature), static adsorption experiments on Cr(VI) are carried out. In each group of experiments, a certain amount of chromium standard solution is taken into glass bottles, diluted to a suitable concentration with deionized water, adjust pH with HCl (1.0 mol.L^{-1}) and NaOH (1.0 mol.L^{-1}). Finally, biochar is added, and the reaction temperature and time are controlled. After ultrasound for 30 min, the reaction is carried out in a constant temperature shaker. After the reaction, a pinhead filter filters part of the solution, and the concentration of Cr(VI) in the filtrate is determined by photometry.

Analysis of the Cr(VI) content in the liquid phase: Transfer the filtered solution shaken well into a glass bottle with a pipette, add 0.5 mL sulfuric acid solution and 0.5 mL 1+1 phosphoric acid solution, and shake up. Add 2 mL color developing agent (I) and shake up. After a period of time, use a 10 mm colorimetric dish to measure the absorbance of the sample at the wavelength of 540 nm. After deducting the absorbance of the blank experiment, the content of Cr(VI) can be obtained from the calibration curve. Calculate the Cr(VI) content in the liquid phase according to the calibration curve.

RESULTS AND DISCUSSION

Sorption Kinetics

Fig. 1 shows the adsorption kinetics of Cr(VI) by biochar under different initial Cr(VI) concentrations, and the overall trend is similar. According to Fig. 1(A), the adsorption of Cr(VI) by biochar increases with time. Due to the many adsorption sites on the biochar surface, the adsorption of Cr(VI) by biochar increases rapidly in the first 20 min. As the adsorption reaction proceeds, the point sites on the biochar surface tend to be saturated. The adsorption rate mainly

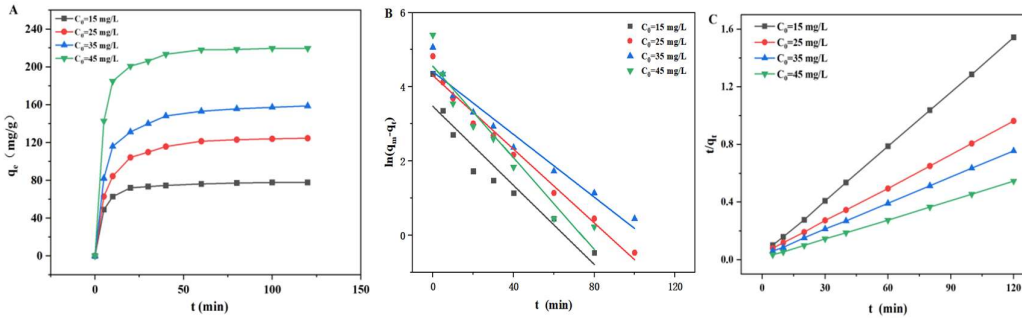

Fig. 1: Results of the dynamic adsorption experiment under different concentration conditions: Results of adsorption amount of biochar on Cr(VI) at different concentrations (A), Results of the first-order dynamic fitting curve (B), Results of the second-order dynamic fitting curve (C).

Table 1: Results of experimental adsorption kinetics at different concentrations.

Conditions	Pseudo-first-order model			Pseudo-second-order model		
	q_e [mg.g^{-1}]	K_1 [h^{-1}]	R^2	q_e [mg.g^{-1}]	K_2 [mg·mg^{-1}.h^{-1}]	R^2
C_0=15 mg.L^{-1}	32.254	0.05322	0.90497	79.6178	4.750	0.99995
C_0=25 mg.L^{-1}	74.135	0.04963	0.97972	130.3781	1.474	0.99991
C_0=35 mg.L^{-1}	82.122	0.04225	0.9542	165.0165	1.247	0.99993
C_0=45 mg.L^{-1}	95.238	0.06175	0.9286	224.7191	1.866	0.99993

depends on the speed of Cr(VI) entering the internal point sites, and the adsorption rate decreases gradually (Chen et al. 2017). After 100 min, the adsorption amount is unchanged with time, and the reaction reaches adsorption equilibrium. The maximum adsorption amount of biochar on 15, 25, 35, and 45 $mg.L^{-1}$ Cr(VI) are 77.726, 124.515, 158.783, and 219.657 $mg.g^{-1}$. Due to the short time required to reach equilibrium, the adsorption of Cr(VI) by biochar is mainly a chemical reaction (Chawla et al. 2016). In the follow-up experiment, the contact time is at least 100 min to achieve a complete adsorption balance.

To obtain more information on the adsorption mechanism of Cr(VI), two models (equations (1) and (2)), the quasi-first-order kinetic model and the quasi-second-order kinetic equation, are used to study the kinetic adsorption process of Cr(VI):

$$\ln (q_m - q_t) = \ln q_e - k_1 t \quad \ldots(1)$$

$$\frac{t}{q_t} = \frac{1}{k_2 q_e^2} + \frac{t}{q_e} \quad \ldots(2)$$

q_t ($mg.g^{-1}$) represents the adsorption capacity of Cr(VI) by biochar at adsorption equilibrium, and q_e ($mg.g^{-1}$) represents the adsorption capacity of Cr(VI) by biochar at adsorption time t. k_1 (h^{-1}) and k_2 ($mg{\cdot}mg^{-1}.h^{-1}$) are the rate constants of the quasi-first-order and quasi-second-order kinetic equations. The experimental data of different initial concentrations of Cr(VI) are fitted and analyzed, and the results are shown in Fig. 1 B and C, respectively. The fitting parameters of adsorption kinetics are listed in Table 1. According to Table 1, when fitting the experimental data with the quasi-second-order kinetic model, the correlation coefficient (R^2) reached 0.99995, much higher than the fitting data of the quasi-first-order kinetic model. Therefore, the adsorption characteristics of Cr(VI) by biochar are more consistent with the quasi-second-order kinetic model, which indicates that the adsorption of Cr(VI) by biochar is mainly based on the chemisorption of ion exchange and chelation reaction between surface compounds and activated functional groups on biochar (Herath et al. 2021).

Adsorption Isotherms at Different Temperatures

Fig. 2 shows the thermodynamic curves of biochar adsorption of Cr(VI) at different temperatures. According to Fig. 2(A), the adsorption capacity of Cr(VI) on biochar gradually increases with the increase of system temperature, indicating that high temperature is conducive to the adsorption of Cr(VI) and biochar adsorption of Cr(VI) is a spontaneous endothermic process. To further obtain the influence of biochar surface on adsorption, Langmuir and Freundlich models (equations 3 and 4) are used for the fitting analysis of isotherms, respectively:

$$\frac{c_e}{q_e} = \frac{c_e}{q_{max}} + \frac{1}{k_l q_{max}} \quad \ldots(3)$$

$$\lg q_e = \lg k_f + \frac{1}{n} \lg c_e \quad \ldots(4)$$

Herein, q_e ($mg.g^{-1}$) is the adsorption amount of Cr(VI) by biochar when the adsorption reaction reaches equilibrium, and c_e ($mg.L^{-1}$) is the concentration of Cr(VI) in the solution after the adsorption reaches the equilibrium. 1/n is the Freundlich constant, k_f is the equilibrium constant of the Freundlich adsorption isothermal model, and k_l is the Langmuir adsorption isothermal model (Fan et al. 2009). The results of isotherm fitting analysis at different temperatures are shown in Fig. 2, and the fitting parameters are listed in Table 2. According to Fig. 2 and Table 2, the Freundlich adsorption isotherm model can better describe the adsorption of Cr(VI) by biochar at different temperatures, indicating that the adsorption process of Cr(VI) by biochar is not only single-molecular layer adsorption but multi-layer adsorption from outer layer to the inner layer (Ho & Mckay 2000). A comparison of adsorption amounts of Cr(VI) on biochar with other common adsorbents such as diatomite (108.56 $mg.g^{-1}$), activated carbon (257.64 $mg.g^{-1}$), zeolite (206.37 $mg.g^{-1}$), activated alumina (164.59 $mg.g^{-1}$), revealed that biochar exhibited much higher adsorption than other common adsorbents did. These results demonstrated that the biochar investigated herein could be a promising adsorbent to effectively decontaminate toxic Cr(VI) in wastewater.

Adsorption Isotherms under the Influence of HA and FA

Fig. 3 shows the isothermal adsorption of Cr(VI) of biochar under the influence of HA and FA. According to Fig. 3, the biochar with FA has the largest adsorption of Cr(VI), followed by biochar with HA, and the adsorption amount of Cr(VI) is the lowest without HA or FA addition. The adsorption amount of Cr(VI) of biochar with FA is significantly higher than that of HA, indicating that FA can improve biochar's adsorption performance on Cr(VI). To further obtain the influence of biochar surface on adsorption, the paper fits the isotherms with Langmuir and Freundlich models (equations 3 and 4). The results of the isotherm fitting under the influence of HA and FA are shown in Fig. 3, and the fitting parameters are listed in Table 3. According to Fig. 3 and Table 3, the Freundlich adsorption isotherm model can better describes the adsorption of biochar to Cr(VI) under the influence of different HA and FA, indicating that the adsorption process of Cr(VI) under the influence of HA and FA is not only single-molecular layer adsorption but multi-layer adsorption from outer layer to the inner layer.

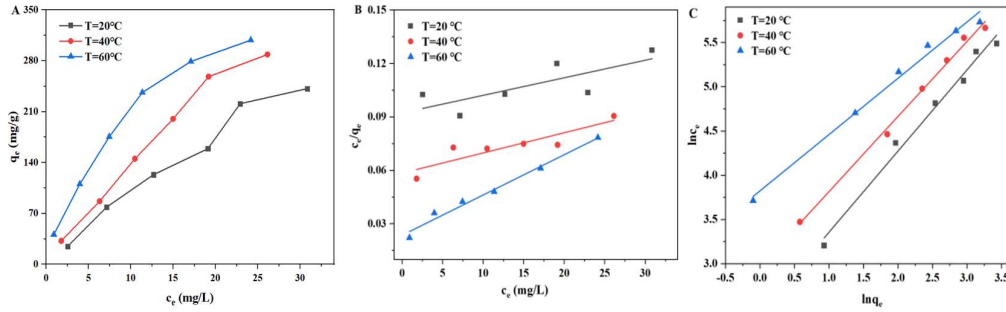

Fig. 2: Adsorption isotherms at different temperatures (A), Langmuir Model fitting result (B), Freundlich Model fitting result (C).

Table 2: Adsorption isotherm fitting results at different temperatures.

Experiment Condition	Langmuir model			Freundlich model		
	q_m [mg.g^{-1}]	K_L [h^{-1}]	R^2	n	K_L [g·mg^{-1}.h^{-1}]	R^2
T=20°C	1014.3572	0.0107	0.59205	1.0898	11.453	0.99047
T=40°C	884.9558	0.0193	0.80384	1.1772	19.417	0.98452
T=60°C	442.4779	0.0959	0.98405	1.5712	45.756	0.99563

Moreover, FA can improve biochar's adsorption performance to Cr(VI) (Deng et al. 2021).

DISCUSSION

FTIR Analysis

Surface properties of the biochar before and after the adsorption of Cr(VI) are characterized and analyzed by FTIR and Raman spectra. The biochar's infrared spectrum (FTIR) is shown in Fig. 4(A). According to Fig. 4(A), the biochar after Cr(VI) adsorption mainly has five characteristic absorption peaks. The peak at ~450 cm^{-1} can be attributed to the complexation between the metal and oxygen, indicating that Cr(VI) successfully adsorption onto the biochar surface. According to the Raman spectra of the biochar before and after the adsorption of Cr(VI), the peak located at ~1350 cm is attributed to the D segment of the defective structural biochar, indicating the disorder and defect degree of the biochar. The peak located at ~1580 cm is attributed to the G segment of the biochar with the sp^2 characteristic structure,

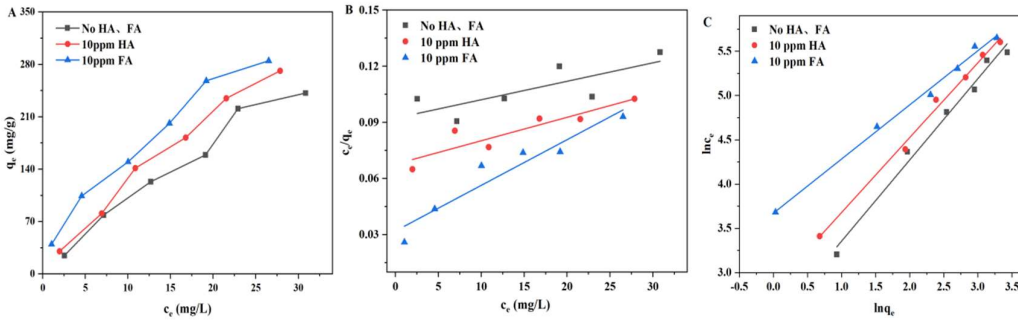

Fig. 3: Adsorption isotherms under the influence of HA and FA (A), Langmuir Model fitting results (B), Freundlich Model fitting results (C).

Table 3: Results of the adsorption isotherms fitting under the influence of HA and FA.

Experiment Condition	Langmuir model			Freundlich model		
	q_m[mg.g^{-1}]	K_L[h^{-1}]	R^2	n	K_L[g·mg.h^{-1}]	R^2
No HA, FA	79.6178	0.3782	0.59205	1.0898	11.453	0.98694
10 mg/L HA	130.3781	0.1922	0.82703	1.1828	17.022	0.99435
10 mg/L FA	165.0165	0.2057	0.91533	1.6348	39.319	0.99484

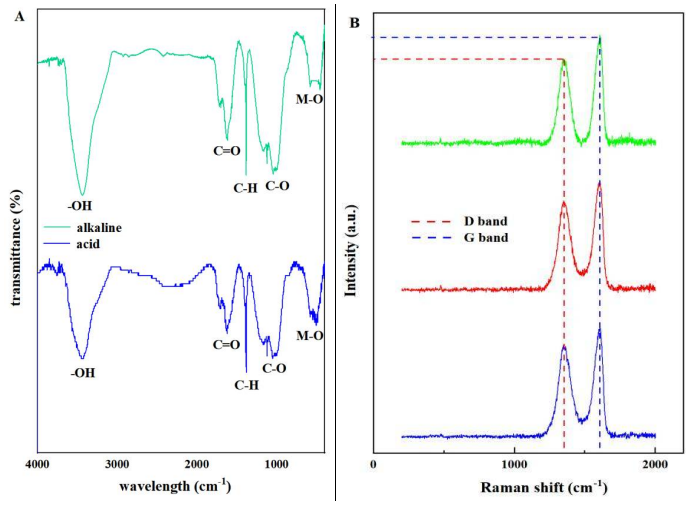

Fig. 4: Infrared spectrogram of Cr(VI) under acid and alkaline conditions (A). Raman spectra before and after Cr(VI) adsorption under acid and alkaline conditions (B).

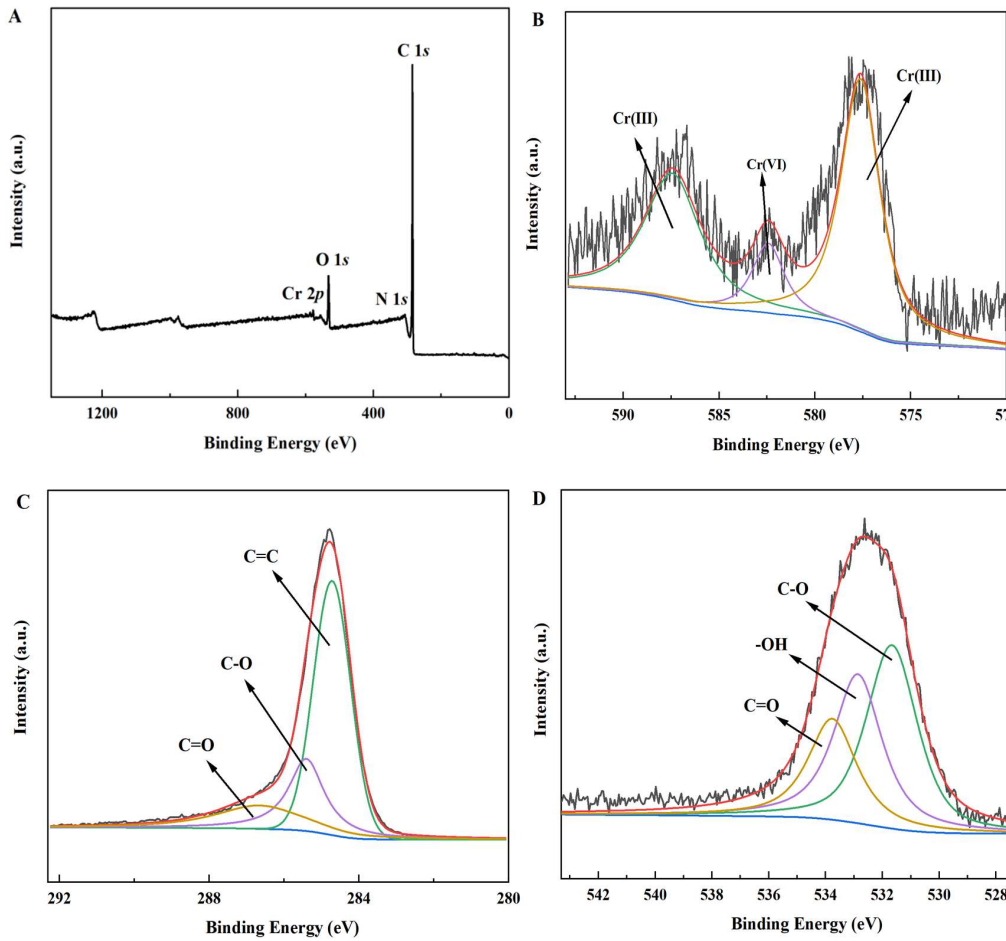

Fig. 5: Full spectrum of biochar after Cr(VI) adsorption (A). Cr 2p XPS Spectrum map (B). C 1s XPS spectra of biochar after Cr(VI) adsorption (C). O 1s XPS spectra of biochar after Cr(VI) adsorption (D).

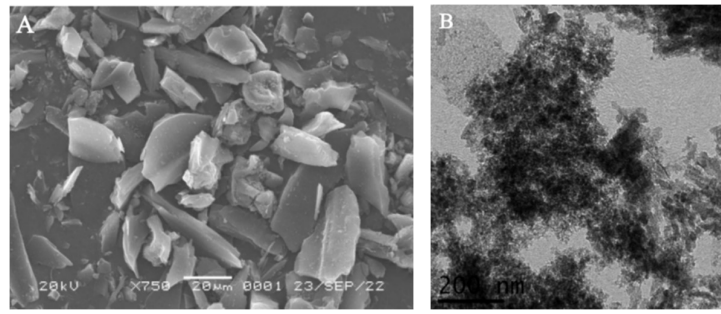

Fig. 6: SEM diagram of the biochar after adsorption of Cr(VI) (A). TEM biochar diagram after Cr(VI) (B) adsorption.

indicating the symmetry and crystallinity of the biochar (Wang et al. 2015). According to Fig. 4(B), the intensity ratio of D and G peaks on Raman spectra differs before and after biochar adsorption. This indicates that the defects and C hybrid structures on the biochar surface have changed after absorbing Cr(VI).

XPS Analysis

The XPS full spectrum of biochar after Cr(VI) adsorption is shown in Fig. 5(A). After adsorption, a new Cr 2p characteristic peak appears, indicating that Cr ions are successfully adsorbed on the surface of biochar (Hou et al. 2020). According to Cr 2p monoelement spectrum (Fig. 5(B)), after the adsorption of Cr(VI), the three peaks produced are two Cr(VI) peaks and one Cr(VI) peak, indicating that biochar reduces part of Cr(VI) to Cr(VI). According to the single element spectrum of C 1s (Fig. 5(C)), there are three types of C, and the peaks at 284.71 eV, 285.40 eV, and 286.65 eV correspond to C=C, C-O, and C=O (Yang et al. 2016). According to the single element spectrum of O 1s (Fig. 5(D)), there are three types of O, and the peaks at 531.67 eV, 532.86 eV, and 533.77 eV correspond to C-O, -OH, and C=O (Wilson & Langell 2014).

SEM and TEM Analysis

Employing scanning electron microscope (SEM) and transmission electron microscope (TEM) to gain the morphology and structure of biochar after the adsorption of Cr(VI), and the results are shown in Fig. 6. According to Fig. 6(A), biochar is composed of many irregular blocks, which are about 10-50 μm long. According to Fig. 6(B), after Cr(VI) adsorption, there are a large number of network materials on the surface of biochar, indicating that Cr(VI) is adsorbed on the biochar surface, and some new reticular substances are formed.

CONCLUSION

Selecting biochar as the adsorbent material, the paper studies the removal performance, influencing factors, and adsorption mechanism of Cr(VI) by static and characterization methods. The results are as follows:

(1) Biochar has a strong adsorption capacity for Cr(VI), and the adsorption reaches a dynamic equilibrium at ~100 min. Moreover, the quasi-second-order kinetic model can better describe the dynamics of Cr(VI), indicating that the adsorption of Cr(VI) by biochar is mainly the chemisorption of ion exchange and chelation reactions between activated functional groups.

(2) Isotherm analysis shows that the adsorption of Cr(VI) is a spontaneous heat absorption process and more in line with the Freundlich equation, indicating that the adsorption process is mainly multilayer adsorption from the outer layer to the inner layer. The adsorption amount of Cr(VI) of biochar with FA is significantly higher than that of HA, indicating that FA can improve biochar's adsorption performance to Cr(VI).

(3) The characterization analysis shows that after the adsorption of Cr(VI), the biochar surface's defect structure and C atomic hybrid structure are changed. Biochar reduces part of Cr(VI) into Cr(III). After the adsorption of Cr(VI) on the surface of biochar, some new substances similar to the network are formed.

REFERENCES

Chawla, A., Prasad, M., Goswami, R., Ranshore, S., Kulshreshtha, A. and Kumar S.A.S. 2016. Kinetic model for sorption of divalent heavy metal ions on low-cost minerals. Korean. J. Chem. Eng., 33(2): 649-656.

Chen, L., Zhou, S.L., Shi, Y.X., Wang, C.H., Li, B.J., Li, Y. and Wu, S.H. 2018. Heavy metals in food crops, soil, and water in the Lihe River watershed of the Taihu Region and their potential health risks when ingested. Sci. Total Environ., 615:141-149.

Chen, N., Kang, M.M., Jiang, X., Wang, H.S., Jia, X.F. and Ji, Y.X. 2017. Study on adsorption mechanism of Cr(VI) from aqueous solutions on biochar produced from coconut shell. Environ. Sci. Manag., 42(12): 66-69.

Deng, C.Y., Lü, J.W. and Chen Z.Y. 2021. Adsorption kinetics and thermodynamics analysis of U(VI) by microbial putrefaction. J. Univ. South China, 35(3): 56.

Fan, Q.H., Shao, D.D., Lu, Y., Wu, W.S. and Wang, X.K. 2009. Effect of

pH, ionic strength, temperature, and humic substances on Ni(II) sorption to Na- attapulgite. Chem. Eng. J., 150(1): 188-195.

Herath, A., Laynea, C., Perezb, F., Hassanc, E.B., Pittmana, C.U. and Mlsnaa, T. 2021. KOH-activated high surface area Douglas fir biochar for adsorbing aqueous Cr(VI). Chemosphere, 269: 128409.

Ho, Y.S. and Mckay, G. 2000. The kinetics of sorption of divalent metal ions onto sphagnum moss flat. Water Res., 34(3): 735-742.

Hou, S.Z., Tian, H.R., Huang, C., Wang, P., Zeng, Q.J., Peng, H.L., Liu, S.L. and Li, A. 2020. Removal of Cr(VI) from aqueous solution by amino-modified biochar supported nano zero-valent iron. Acta Sci. Circum., 40(11): 3931-3938.

Lyu, H., Tang, J., Huang, Y., Gai, L., Zeng, E.Y., Liber, K. and Gong, Y. 2017. Remove hexavalent chromium from aqueous solutions by a novel biochar-supported nanoscale iron sulfide composite. Chem. Eng. J., 322: 516-524.

Lyu, H., Zhao, J., Tang, Y., Gong, Y., Huang, Q., Wu, B. and Gao, G. 2018. Immobilization of hexavalent chromium in contaminated soils using biochar-supported nanoscale iron sulfide composite. Chemosphere, 194: 360-369.

Mian, M.M. and Liu, G.J. 2018. Recent progress in biochar-supported photocatalysts: synthesis, the role of biochar, and applications. RSC Adv., 8(26): 14237-14248.

Wang, F.F., Wang, F., Gao, G.D. and Chen, W. 2015. Transformation of graphene oxide by ferrous iron: environmental implications. Environ. Toxicol. Chem., 34(9): 1975-1982.

Wang, K.X., Tang, X.H., Liu, L., Yao, S.S., Pu, Y., Zhao, F. and Chen, Q.Y. 2022. Adsorption of Cr(VI) from water by modified tea residue biochar. Shandong Chem. Ind., 51(21): 5-10.

Wilson, D. and Langell, M.A. 2014. XPS analysis of oleylamine/oleic acid capped Fe_3O_4 nanoparticles as a function of temperature. Appl. Surf. Sci., 303: 6-13.

Yang, J.P., Zhao, Y.C., Ma, S.M., Zhu, B.B., Zhang, J.Y. and Zheng, C.G. 2016. Mercury removal by magnetic biochar derived from simultaneous activation and magnetization of sawdust. Environ. Sci. Technol., 50(21): 12040-12047.

Zou, H.W., Zhao, J.W., He, F., Zhong, Z., Huang, J.S., Zheng, Y.L., Zhang, Y., Yang, Y.C., Yu, F., Bashir, M.A. and Gao, B. 2021. Ball milling biochar iron oxide composites for the removal of chromium (Cr(VI)) from water: Performance and mechanisms. J. Hazard. Mater., 413: 125252.